American Journal of Applied Mathematics
2020; 8(5): 257-264
http://www.sciencepublishinggroup.com/j/ajam
doi: 10.11648/j.ajam.20200805.13
ISSN: 2330-0043 (Print); ISSN: 2330-006X (Online)

Numerical Solution of Elastohydrodynamic Lubrication for Sliding/Rolling Bearing for Non-newtonian Lubricant

Samuel Macharia Karimi[1, *], Mark Kimathi[2], Mathew Ngugi Kinyanjui[3]

[1]Pan African University, Institute of Basic Sciences, Technology and Innovation, Nairobi, Kenya

[2]Department of Mathematics, Statistics and Actuarial Science, Machakos University, Machakos, Kenya

[3]Department of Pure and Applied Mathematics, Jomo Kenyatta University of Agriculture and Technology, Nairobi, Kenya

Email address:
karimimacharia@gmail.com (S. M. Karimi)

[*]Corresponding author

To cite this article:
Samuel Macharia Karimi, Mark Kimathi, Mathew Ngugi Kinyanjui. Numerical Solution of Elastohydrodynamic Lubrication for Sliding/Rolling Bearing for Non-Newtonian Lubricant. *American Journal of Applied Mathematics.* Vol. 8, No. 5, 2020, pp. 257-264.
doi: 10.11648/j.ajam.20200805.13

Received: August 12, 2020; **Accepted**: September 3, 2020; **Published**: September 11, 2020

Abstract: There is always a demand in the industry sector to increase the efficiency of machine components to reduce wear and tear. This paper presents the numerical solution to the study of Elastohydrodynamic lubrication point contact for sliding/rolling bearing where the viscosity of the lubricant is non-Newtonian. The assumption that a lubricant is Newtonian reduces validation of the model hence the Reynolds-Eyring model in this research will incorporate the non-Newtonian nature of the lubricant of the bearing. The mathematical model comprises of Reynold-Eyring equation, film thickness, load balance, lubricant viscosity and lubricant density equations together with their boundary conditions. The Reynolds-Eyring equation governing the flow is non-linear hence the finite difference method numerical technique is used to discretize it together with the other two dimensional equations. These equations are solved simultaneously and Matlab software is used simulate the results. The film thickness and pressure profiles with various loads and speeds are presented. The findings note that an increase in load lowers the pressure and film thickness while an increase in the speed results to a direct increase in pressure and film thickness. A pressure spike is also noted at the exit of the bearing.

Keywords: Elastohydrodynamic, Thermal, Eyring, Non-newtonian

1. Introduction

Lubrication is an important aspect for modern machine so that they can work efficiently and have long life. The use of a lubricant between two surfaces in contact reduces the friction and the wear. Elastohydrodynamic lubrication (EHL) is an important aspect of research in lubrication theory primarily in heavily loaded contacts. This type of lubrication considers deformation of the bearing contacts. Goodyer [1] in his research in adaptive numerical methods for elastohydrodynamic lubrication was able to get numerical solutions for his mathematical model using the Reynolds equation. The Reynolds equation which was derived by Osborn combines both the continuity and momentum equations to a single equation that describes the pressure of fluid [2].

Most lubricants are non-Newtonian. Most research has modelled using Newtonian lubricants because of the straightforward and simple constitutional expression in the Reynolds equation. Previous research has shown that non-Newtonian lubricants greatly affect the film thickness [3]. Many rheological models have been proposed to incorporate the non-Newtonian nature of lubricants during mathematical modelling. They include the Reynolds-Eyring model, Johnson-Tevaarwerk model, power-law model among others [4]. Most researchers have recommended the Reynolds-Eyring model for traction studies and lubrication performance studies [5]. Liu [6] in his research was able to derive the Reynolds-Eyring equation for line contacts. This research extends his work to point contacts.

Since EHL experiments are still expensive and difficult to

conduct in the lab, numerical simulations have been important tool for research in EHL. There are many numerical techniques which have been used to solve EHL problems. The direct method, inverse method, finite element method, finite difference method, multigrid method, computer fluid dynamics (CFD), among others [7, 8, 9]. The study [10] used the numerical finite difference technique to discretise the Reynolds equation and the viscosity equation for the rheology model in their research. The research study [11] solved both the Reynolds and energy equation using the finite difference method. The numerical study [12] and [13] in their research of hydrodynamic lubrication of an inclined pad thrust bearing used the finite difference method to solve both the pressure and energy equations. Thus in this paper, the Reynolds-Eyring model will be solved using the finite difference method.

2. Mathematical Formulation

The Analysis of Non-Newtonian Elastohydrodynamic lubrication flow for point contacts has not been analyzed extensively. This research focusses on two dimensional (point contacts) numerical solution for Elastohydrodynamic lubrication for a sliding/rolling bearing where the non-Newtonian aspect of the lubricant will be put into consideration. The lubricant flow is considered to be in the x and y direction as demonstrated in figure 1. Due to heavy loads and pressure, the bearing surfaces deforms as illustrated in figure 2.

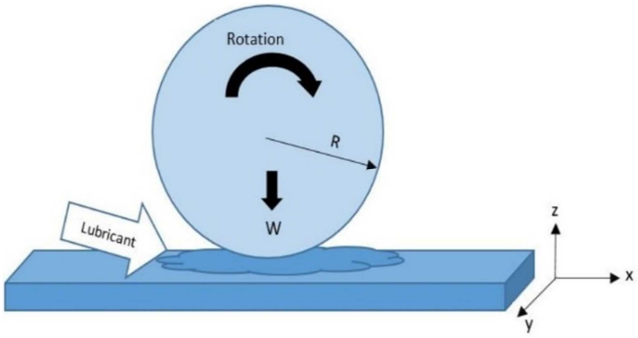

Figure 1. *Geometry before deformation.*

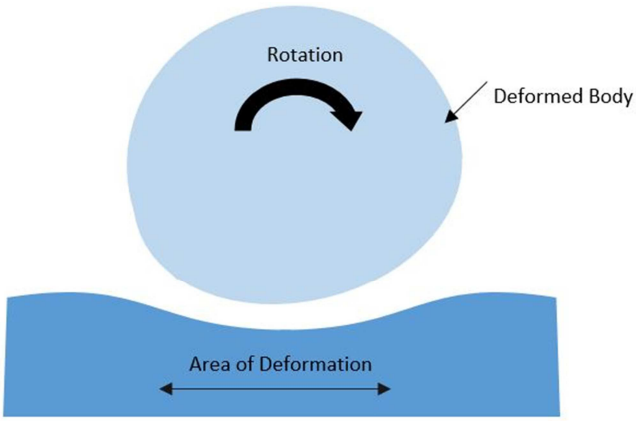

Figure 2. *Geometry after deformation.*

3. Governing Equations

The main equations governing the flow are the Reynold-Eyring, film thickness, lubricant viscosity, lubricant density equations. Point contact Elastohydrodynamic lubrication analysis is considered in this research. In rectangular coordinates, the general equations for the flow are given by

3.1. Non-Newtonian Model

In this paper, to incorporate non-Newtonian nature of the lubricant the Eyring model is used [6].

$$\gamma = \frac{\tau_0}{\eta} sinh\left(\frac{\tau}{\tau_0}\right) \tag{1}$$

The Eyring model in both the x and y direction can be given by,

$$\frac{\partial u}{\partial z} = \frac{\tau_0}{\eta} sinh\left(\frac{\tau_{zx}}{\tau_0}\right), \frac{\partial v}{\partial z} = \frac{\tau_0}{\eta} sinh\left(\frac{\tau_{zy}}{\tau_0}\right) \tag{2}$$

3.2. Reynolds-Eyring Equation

The Navier stokes equation with the usual assumptions in the x and y direction reduces to,

$$\frac{\partial p}{\partial x} = \frac{\partial(\tau_{zx})}{\partial z}, \frac{\partial p}{\partial y} = \frac{\partial(\tau_{zy})}{\partial z} \tag{3}$$

If we assume that pressure is a function of x alone, we integrate the first equation of (3) with respect to z to get

$$\tau_{zx} = \frac{\partial p}{\partial x} z + C_1 \tag{4}$$

where C_1 is a constant of integration

Substituting equation (4) in the first equation of equations (2)

$$\frac{\partial u}{\partial z} = \frac{\tau_0}{\eta} \sinh\left[\frac{1}{\tau_0}\left(\frac{\partial p}{\partial x} z + C_1\right)\right] \tag{5}$$

Integrating equation (5) with respect to u and z with C_2 as a constant of integration

$$u = \frac{{\tau_0}^2}{\eta \frac{\partial p}{\partial x}} cosh\left[\frac{1}{\tau_0}\left(\frac{\partial p}{\partial x} z + C_1\right)\right] + C_2 \tag{6}$$

Now applying the boundary condition on the lower plate i.e. at z=0; u=U_1, equation (6) becomes

$$U_1 = \frac{{\tau_0}^2}{\eta \frac{\partial p}{\partial x}} cosh\left[\frac{C_1}{\tau_0}\right] + C_2 \tag{7}$$

Substituting the value of C_2 given by equation (7) into equation (6)

$$u = U_1 + \frac{{\tau_0}^2}{\eta \frac{\partial p}{\partial x}}\left[cosh\left[\frac{1}{\tau_0}\left(\frac{\partial p}{\partial x} z + C_1\right)\right] - cosh\left[\frac{C_1}{\tau_0}\right]\right] \tag{8}$$

Taking τ_m to be the shear stress of the mid plane at z=0.5h and from equation (4)

$$\tau_m = \frac{h}{2}\frac{\partial p}{\partial x}z + C_1 \tag{9}$$

With

$$\xi = \frac{h}{2\tau_0}\frac{\partial p}{\partial x}, \delta = \frac{h}{2\tau_0}\frac{\partial p}{\partial y} \tag{10}$$

Substituting equations (9) and (10) into equation (8)

$$u = U_1 + \frac{h\tau_0}{2\eta\xi}\left[cosh\left[\frac{\tau_m}{\tau_0} - \xi + \frac{2z\xi}{h}\right] - cosh\left[\frac{\tau_m}{\tau_0} - \xi\right]\right] \tag{11}$$

Similarly, in the y-direction we get

$$v = V_1 + \frac{h\tau_0}{2\eta\delta}\left[cosh\left[\frac{\tau_m}{\tau_0} - \delta + \frac{2z\delta}{h}\right] - cosh\left[\frac{\tau_m}{\tau_0} - \delta\right]\right] \tag{12}$$

Applying the boundary condition at the upper plate i.e. z=h; u=U_2 and v=V_2 on equation (11) and equation (12) we get

$$U_2 = U_1 + \frac{h\tau_0}{2\eta\xi}\left[cosh\left[\frac{\tau_m}{\tau_0} + \xi\right] - cosh\left[\frac{\tau_m}{\tau_0} - \xi\right]\right] \tag{13}$$

$$V_2 = V_1 + \frac{h\tau_0}{2\eta\delta}\left[cosh\left[\frac{\tau_m}{\tau_0} + \delta\right] - cosh\left[\frac{\tau_m}{\tau_0} - \delta\right]\right] \tag{14}$$

Applying the following identity

$$\cosh(x+y) - \cosh(x-y) = 2\sinh(x)\sinh(y)$$

in equation (13) and (14), we get the following, respectively

$$\sinh\left(\frac{\tau_m}{\tau_0}\right)\sinh(\xi) = \frac{\eta\xi}{\tau_0 h}(U_2 - U_1) \tag{15}$$

$$\sinh\left(\frac{\tau_m}{\tau_0}\right)\sinh(\delta) = \frac{\eta\delta}{\tau_0 h}(V_2 - V_1) \tag{16}$$

Substituting the values of u and v from equations (11) into two dimensional continuity equation

$$\frac{\partial\rho}{\partial t} + \frac{\partial(\rho u)}{\partial x} + \frac{\partial(\rho v)}{\partial y} = 0 \tag{17}$$

$$\frac{\partial}{\partial x}\left[\rho U_1 + \frac{\rho h\tau_0}{2\eta\xi}\left[cosh\left[\frac{\tau_m}{\tau_0} - \xi + \frac{2z\xi}{h}\right] - cosh\left[\frac{\tau_m}{\tau_0} - \xi\right]\right]\right] + \frac{\partial}{\partial y}\left[\rho V_1 + \frac{\rho h\tau_0}{2\eta\delta}\left[cosh\left[\frac{\tau_m}{\tau_0} - \delta + \frac{2z\delta}{h}\right] - cosh\left[\frac{\tau_m}{\tau_0} - \delta\right]\right]\right] + \frac{\partial\rho}{\partial t} = 0 \tag{18}$$

Now, integrating equation (18) with respect to z from z=0 to z=h and using the identity

$$\cosh(A-B) = \cosh(A)\cosh(B) - \sinh(A)\sinh(B)$$

then substituting equations (14) we get

$$\frac{\partial\rho h}{\partial t} - \frac{\partial}{\partial x}\left[\frac{\rho h^3}{12\eta}\frac{\partial p}{\partial x}\left[\frac{3(\xi\cosh(\xi) - \sinh(\xi))}{\xi^3}cosh\left[\frac{\tau_m}{\tau_0}\right]\right]\right] - \frac{\partial}{\partial y}\left[\frac{\rho h^3}{12\eta}\frac{\partial p}{\partial y}\left[\frac{3(\delta\cosh(\delta) - \sinh(\delta))}{\delta^3}cosh\left[\frac{\tau_m}{\tau_0}\right]\right]\right] +$$

$$\frac{\partial}{\partial x}\left[\frac{U_1+U_2}{2}\rho h\right] + \frac{\partial}{\partial y}\left[\frac{V_1+V_2}{2}\rho h\right] = 0 \tag{19}$$

Assuming that there is no tangential direction and U_m=U_1+U_2 and V_m=V_1+V_2, the Reynold's-Eyring equation becomes

$$\frac{\partial}{\partial x}\left[\frac{\rho h^3}{12\eta}\frac{\partial p}{\partial x}S(x)\right] + \frac{\partial}{\partial y}\left[\frac{\rho h^3}{12\eta}\frac{\partial p}{\partial y}\,Q(y)\right] = \frac{U_m}{2}\frac{\partial(\rho h)}{\partial x} + \frac{V_m}{2}\frac{\partial(\rho h)}{\partial y} + \frac{\partial\rho h}{\partial t} \tag{20}$$

Where

$$S(x) = \frac{3(\xi\cosh(\xi) - \sinh(\xi))}{\xi^3}cosh\left[\frac{\tau_m}{\tau_0}\right]$$

$$Q(y) = \frac{3(\delta\cosh(\delta) - \sinh(\delta))}{\delta^3}cosh\left[\frac{\tau_m}{\tau_0}\right]$$

The shear stress τ_0 represents the change of the lubricant from Newtonian to non-Newtonian. As τ_0 approaches infinity, the parameters ξ and δ approach zero and by L' Hopitals rule S (x) and Q (y) will be unitary. Thus Equation (20) becomes Reynolds Newtonian equation.

Substituting into equation (15) and (16) the hyperbolic identity

$$sinh^2 x = 1 + cosh^2 x$$

$$cosh\left[\frac{\tau_m}{\tau_0}\right] = \sqrt{1 + \left[\frac{\eta(U_2-U_1)}{\tau_0 h}\frac{\xi}{\sinh(\xi)}\right]^2} \tag{21}$$

Substituting equation (21) into S (x) and Q (y) above

$$S(x) = \frac{3(\xi\cosh(\xi)-\sinh(\xi))}{\xi^3}\sqrt{1+\left[\frac{\eta(U_2-U_1)}{\tau_0 h}\frac{\xi}{\sinh(\xi)}\right]^2} \tag{22}$$

$$Q(y) = \frac{3(\delta\cosh(\delta)-\sinh(\delta))}{\delta^3}\sqrt{1+\left[\frac{\eta(V_2-V_1)}{\tau_0 h}\frac{\delta}{\sinh(\delta)}\right]^2} \tag{23}$$

3.3. Film Thickness Equation

The film thickness equation for point contact with surface roughness

$$h(x,y) = h_{00} + \frac{x^2}{2R} + \frac{y^2}{2R} + s_r(x,y) + \frac{2}{\pi E'}\int_{-\infty}^{\infty}\int_{-\infty}^{\infty}\frac{p(x',y')}{\sqrt{(x-x')^2+(y-y')^2}}dx'\,dy' \tag{24}$$

3.4. Lubricant Viscosity Equation

The lubricant viscosity is assumed to be dependent on pressure which is given by Roelands [14]

$$\eta = \eta_0 e^{\ln(\eta_0)+9.67[-1+(1+5.1\times10^{-9}p)^Z]} \tag{25}$$

3.5. Lubricant Density Equation

Due to high pressures, the compressibility of the lubricant has to be considered. The lubricant density is assumed to be dependent on pressure hence most the Barus model is used since it is valid even for high pressures [15].

$$\rho = \rho_0\left[1+\frac{0.6\times10^{-9}p}{1+1.7\times10^{-9}p}\right] \tag{26}$$

3.6. Non-Dimensionalization

The equations are non-dimensionalized using the Hertzian dry contact variables below [16].

$$\bar{\rho} = \frac{\rho}{\rho_0}, \bar{\eta} = \frac{\eta}{n_0}, P = \frac{p}{p_h}, X = \frac{x}{a}, Y = \frac{y}{a}, H = \frac{hR}{a^2},$$

$$T = \frac{tu}{2a}, H_{00} = \frac{h_{00}R}{a^2}, U = \frac{u_m\eta_0}{RE'}, V = \frac{v_m\eta_0}{RE'}, \mathrm{R} = \frac{s_r R}{a^2}$$

3.6.1. Dimensionless Reynold-Eyring Equation

Applying the above non-dimensionless variables to the Reynold-Eyring equation becomes and assuming the rolling speed U_m=V_m in the x and y direction is the same we have,

$$\frac{\partial}{\partial X}\left[\frac{\bar{\rho}H^3}{\bar{\eta}}\frac{\partial P}{\partial X}S(X)\right] + \frac{\partial}{\partial Y}\left[\frac{\bar{\rho}H^3}{\bar{\eta}}\frac{\partial P}{\partial Y}\,Q(X)\right] = \lambda\left[\frac{\partial(\bar{\rho}H)}{\partial X} + \frac{\partial(\bar{\rho}H)}{\partial Y} + \frac{\partial\bar{\rho}H}{\partial T}\right] \tag{27}$$

With

$$S(x) = \frac{3(\xi\cosh(\xi)-\sinh(\xi))}{\xi^3}\sqrt{1+\left[\frac{Rn_0\bar{\eta}(U_2-U_1)}{\tau_0 Ha^2}\frac{\xi}{\sinh(\xi)}\right]^2}$$

$$Q(y) = \frac{3(\delta\cosh(\delta)-\sinh(\delta))}{\delta^3}\sqrt{1+\left[\frac{Rn_0\bar{\eta}(V_2-V_1)}{\tau_0 Ha^2}\frac{\delta}{\sinh(\delta)}\right]^2}$$

$$\lambda = \frac{6\eta_0 UR^2}{p_h a^3}, \xi = \frac{Hap_h}{2R\tau_0}\frac{\partial P}{\partial X}, \delta = \frac{Hap_h}{2R\tau_0}\frac{\partial P}{\partial Y}$$

If we let

$$\beta = \frac{\bar{\rho}H^3}{\bar{\eta}}$$

The Reynold-Eyring equation (27) becomes

$$\frac{\partial}{\partial X}\left[\beta\frac{\partial P}{\partial X}S(X)\right] + \frac{\partial}{\partial Y}\left[\beta\frac{\partial P}{\partial Y}\,Q(X)\right] = \lambda\left[\frac{\partial(\bar{\rho}H)}{\partial X} + V_m\frac{\partial(\bar{\rho}H)}{\partial Y} + \frac{\partial\bar{\rho}H}{\partial T}\right] \tag{28}$$

3.6.2. Dimensionless Film Thickness Equation

$$H(x,y) = H_{00} + \frac{X^2}{2} + \frac{Y^2}{2} + \mathrm{R}\,(X,Y) + \frac{2}{\pi^2}\int_{-\infty}^{\infty}\int_{-\infty}^{\infty}\frac{P(X',Y')}{\sqrt{(X-X')^2+(Y-Y')^2}}\,dX'\,dY' \tag{29}$$

3.6.3. Dimensionless Lubricant Viscosity Equation

$$\bar{\eta} = e^{\ln(\eta_0)+9.67[-1+(1+5.1\times10^{-9}Pp_h)^Z]} \tag{30}$$

3.6.4. Dimensionless Lubricants Density Equation

$$\bar{\rho} = \left[1 + \frac{0.6\times10^{-9}Pp_h}{1+1.7\times10^{-9}Pp_h}\right] \tag{31}$$

3.7. Boundary Conditions

The model equations are discretised on a rectangular domain $X_{in} \le X \le X_{end}$ and $Y_{in} \le Y \le Y_{end}$
The boundary conditions in accordance to [18] are given by

$$P(X_{in},Y) = 0, P(X_{end},Y) = 0, P(X,Y_{in}) = 0, P(X,Y_{end}) = 0$$

$$\frac{\partial P}{\partial X_{end}} = \frac{\partial P}{\partial Y_{end}} = 0$$

4. Numerical Solution

The Reynolds-Eyring equation is non-linear partial differential equation which cannot be solved analytically. Therefore, the finite difference numerical method is used to approximate the solutions of this equation together with other equations affecting the flow of lubricant. The partial derivatives are replaced by two dimensional finite-sized difference nodes at particular locations of a solution mesh. This reduces the problem to a system of linear equations which can be solved by an iteratively [17]. Reynolds-Eyring equation after discretization after and making $P_{i,j}$ the subject of the formula becomes

$$P_{i,j} = \left[\begin{array}{c}\frac{1}{(dx)^2}\left(\beta_{i-\frac{1}{2},j}P_{i-1,j}S_{i-\frac{1}{2},j} + \beta_{i+\frac{1}{2},j}P_{i+1}S_{i+\frac{1}{2},j}\right) + \frac{1}{(dy)^2}\left(\beta_{i,j-\frac{1}{2}}P_{i,j-1}S_{i,j-\frac{1}{2}} + \beta_{i,j+\frac{1}{2}}P_{i,j+1}S_{i,j+\frac{1}{2}}\right)\\ -\frac{\lambda}{dx}\left(H_{i,j}\bar{\rho}_{i,j} - H_{i-1,j}\bar{\rho}_{i-1,j}\right) - \frac{\lambda}{dy}\left(H_{i,j}\bar{\rho}_{i,j} - H_{i,j-1}\bar{\rho}_{i,j-1}\right) - \frac{\lambda}{dt}\left(H_{i,j}^{k+1}\bar{\rho}_{i,j}^{k+1} - H_{i,j}^{k}\bar{\rho}_{i,j}^{k}\right)\end{array}\right]$$

$$\div \left[\frac{1}{(dx)^2}\left(\beta_{i-\frac{1}{2},j}S_{i-\frac{1}{2},j} + \beta_{i+\frac{1}{2},j}S_{i+\frac{1}{2},j}\right) + \frac{1}{(dy)^2}\left(\beta_{i,j-\frac{1}{2}}S_{i,j-\frac{1}{2}} + \beta_{i,j+\frac{1}{2}}S_{i,j+\frac{1}{2}}\right)\right] \tag{32}$$

Film thickness equation in discrete form

$$H_{i,j} = H_{00} + \frac{X_{i,j}^2}{2} + \frac{Y_{i,j}^2}{2} + \mathrm{R}_{i,j} + \frac{2}{\pi^2}\sum_{r=0}^{n_x-1}\sum_{s=0}^{n_y-1}K_{r,i,s,j}P_{rs} \tag{33}$$

Where

$$K_{r,i,s,j} = |X_p|sinh^{-1}\left(\frac{Y_p}{X_p}\right) + |Y_p|sinh^{-1}\left(\frac{X_p}{Y_p}\right) - |X_m|sinh^{-1}\left(\frac{Y_p}{X_m}\right) + |Y_p|sinh^{-1}\left(\frac{X_m}{Y_p}\right)$$

$$-|X_p|sinh^{-1}\left(\frac{Y_m}{X_p}\right) + |Y_m|sinh^{-1}\left(\frac{X_p}{Y_m}\right) + |X_m|sinh^{-1}\left(\frac{Y_m}{X_m}\right) + |Y_m|sinh^{-1}\left(\frac{X_m}{Y_m}\right)$$

$$X_p = X_i - X_r + \frac{dx}{2},\ X_m = X_i - X_r - \frac{dx}{2},\ Y_p = Y_j - Y_s + \frac{dy}{2},\ Y_m = Y_j - Y_s - \frac{dy}{2}$$

Lubricant viscosity equation in discrete form

$$\bar{\eta}_{i,j} = e^{\ln(\eta_0)+9.67[-1+(1+5.1\times10^{-9}P_{i,j}p_h)^Z]} \tag{34}$$

Lubricant density equation in discrete form

$$\bar{\rho}_{i,j} = \left[1 + \frac{0.6\times10^{-9}P_{i,j}p_h}{1+1.7\times10^{-9}P_{i,j}p_h}\right] \tag{35}$$

5. Results and Discussion

The following graphs of pressure and film thickness illustrates the effects of several parameters and variables.

5.1. Pressure Profile

It is noted from the figures 3, figure 4 and figure 6 that the pressure increases gradually from the entrance of the bearing. At the centre of the sliding/ rolling bearing, the pressure achieves maximum pressure. Then the pressure decreases steadily at the exit contact. At the centre of the bearing there is greater contact between the rolling element and surface hence higher pressure. The pressure spike occurs at the exit of the sliding/rolling bearing due to cavitation. The cavitation is a result of sudden reduction in pressure which causes the lubricant to form air bubbles.

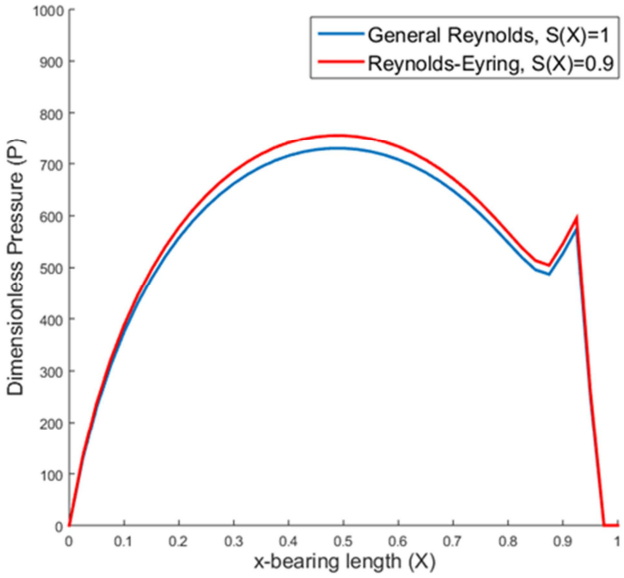

Figure 3. *Effects of Eyring Parameter on Pressure.*

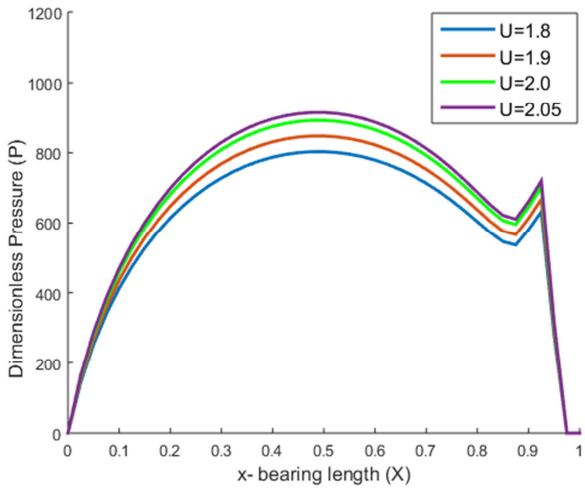

Figure 4. *Effects of Speed on Pressure.*

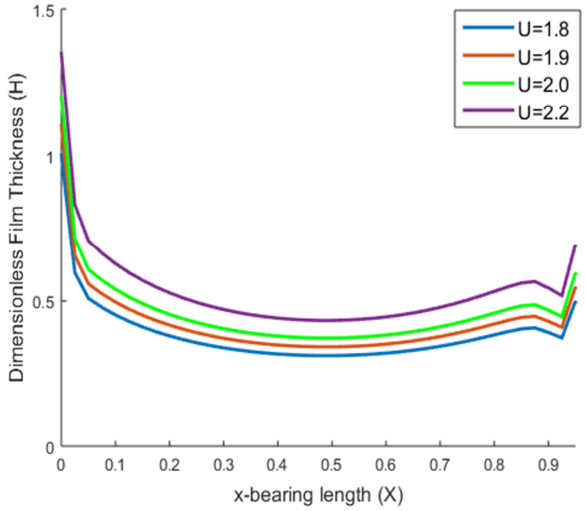

Figure 5. *Effects of Speed on Film Thickness.*

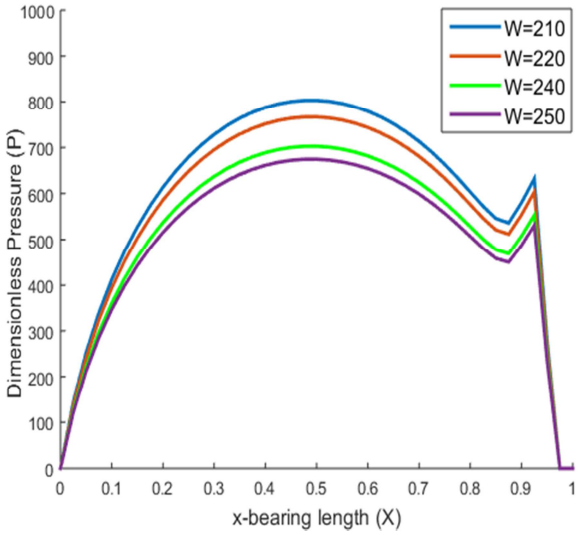

Figure 6. *Effects of Load on pressure.*

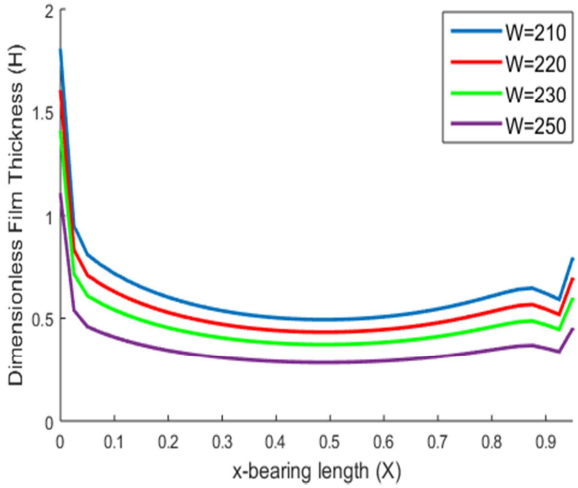

Figure 7. *Effects of Load on Film Thickness.*

5.2. Effect of Eyring Parameter on Pressure

For the Reynolds-Eyring model, the effective viscosity in the x coordinate is given by $\eta_{eff} = \frac{\eta}{S(x)}$. Thus a decrease in the non-Newtonian Parameter S(x) results in the increase of effective viscosity. As shown in Figure 3, this reduction results to increase in the pressure. An increase in the viscosity of the lubricant leads to an increase in the height of the film thickness which in turn increases the pressure. No one lubricant is Newtonian, hence the non-Newtonian model gives better realistic results due to the changes in the viscosity of the lubricant.

5.3. Effects of Speed on Pressure and Film thickness

It is noted from figure 4 that as the speed increases of the rolling element, the pressure also increases. This can be attributed to the fact that the film thickness becomes thicker as the speed of the rolling element increases. It is also known that the relative sliding between the contact surface and rolling element causes temperature increase which affect the components and lubricant properties of the bearing. Thus when the speed of the rolling element increases it leads to the height of the film thickness increasing due to thermal rise.

The film thickness becomes thicker with increase in speed hence an increase in the film thickness as shown in figure 5. As the rolling speed increases, the friction reduces which results to increase in the film thickness and pressure.

5.4. Effects of Load on Pressure and Film Thickness

The figure 6 shows that as the load increases the pressure decreases. Moreover, as the load increases it leads to a reduction in the film thickness height (the film thickness becomes thinner) as shown in figure 7. Increase in load results to decrease in the viscosity of the lubricant which in turn reduces the load carrying capacity ability of the bearing. That at high load the film thickness becomes thinner than at light load. This is due to the fact that as the load increases, the friction of the contact region increases which in turn affects the pressure and film thickness.

The results in this research were compared and validated with other numerical and experimental work in the area of elastohydrodynamic lubrication such as [14, 19-21]. The results obtained agree and compares well. That the film thickness and pressure are affected when the speed and load in the bearing is varied and a pressure peak is noted in the pressure profiles.

6. Conclusion

The numerical solution of Elastohydrodynamic lubrication for sliding/ rolling bearing using non-Newtonian lubricant has been investigated. To incorporate the non-Newtonian nature of the lubricant, the Reynold-Eyring equation has been used. The effects of rolling speed and load on pressure and film thickness have then been discussed. In conclusion, the pressure increases with increase in speed while reduces with increase in load. The film thickness increases with increase in speed of the rolling element and reduces with increase in load. The pressure peak is a result of cavitation.

Nomenclature

γ	Eyring parameter
η	The viscosity of the lubricant
η_0	The viscosity at reference pressure
ρ	The density of the lubricant
ρ_0	Density at reference pressure
τ	Shear stress
τ_0	Eyring shear stress
Z	Viscosity pressure index
x	Distance along x direction
y	Distance along y direction
u	Velocity along x direction
u_m	mean velocity
v	Velocity along y direction
a	Hertzian radius
t	Time
p	Pressure
p_h	Maximum Hertzian pressure
h	Film thickness
h_{00}	Minimum film thickness
s_r	Surface roughness
E'	Young Modulus
R	Radius of rolling element

Acknowledgements

First author would like to thank the Pan African University (PAUSTI) for providing educational and financial support to conduct this research.

References

[1] C. E. Googyer, "Adaptive numerical methods for elastohydrodynamic lubrication", PhD thesis, The University of Leeds School of Computing, May 2001.

[2] A. F. Koura, M. E. Elhady and M. S. Metwally, "Numerical solution of Reynolds equation using differential transform method", International Journal of Advanced Research (IJAR), vol. (6), pp. 729-737, 2018.

[3] D. Dowson, "Modelling of elastohydrodynamic lubrication of real solids by real lubricants", Meccanica, vol. 33, pp. 47-58, 1998.

[4] H. Liu, K. Mao, C. Zhu, X. Xu, and M. Liu, "Parametric studies of spur gear lubrication performance considering dynamic loads", Proceedings of the Institution of Mechanical Engineers, Part J: Journal of Engineering Tribology, May 9, 2012.

[5] Y. -Q. Wang and X.-J. Yi, "Non-Newtonian transient thermoelastohydrodynamic lubrication analysis of an involute spur gear", Lubrication Science, vol. 22, pp. 465-478, 2010.

[6] H. Liu, "Lubricated Contact Analysis of a Spur Gear Pair with Dynamic Loads", PHD Thesis, School of Engineering, University of Warwick April 2013.

[7] H. Lu, M. Berzins, C. E. Goodyer, and P. K. Jimack, "High order discontinuous Galerkin method for elastohydrodynamic lubrication line contact problems", Communications in Numerical Methods in Engineering, vol. 21, pp. 643-650, 2005.

[8] T. Almqvist and R. Larsson, "Thermal transient rough EHL line contact simulations by aid of computational fluid dynamics", Tribology International, vol. 41, pp. 683-693, 2008.

[9] M. Berzins, C. E. Goodyer and P. Jimack, " High order discontinuous Galerkin method for elastohydrodynamic lubrication line contact", Communications in Numerical Methods in Engineering, vol. 00, pp. 1-6, 2000.

[10] Y. Liu, Q. J. Wang, S. Bair, and P. Vergne, "A quantitative solution for the full shear thinning EHL point contact problem including traction", Tribology Letters, vol. 28 (2):171-181, 2007.

[11] D. V. Srikanth, A. N. Kaushal, K. B. Chaturvedi et al., "Determination of a large tilting pad thrust bearing angular stiffness", Tribology International, 47, 69-76, 2012.

[12] P. R. Kiogora, M. N. Kinyanjui, D. M. Theuri, "A Conservative Scheme Model of an Inclined Pad Thrust Bearing", International Journal of Engineering Science and Innovative Technology (IJESIT) Volume 3, Issue 1, January 2014.

[13] P. R. Kiogora, M. N. Kinyanjui, D. M. Theuri, "Numerical Solution of the Momentum and Energy Equations of an Inclined Pad Thrust Bearing", International Journal of Engineering Science and Innovative Technology (IJESIT) Volume 3, Issue 3, May 2014.

[14] V. Petrone, A. Senatore and V. D'Agostino, "Effect of an Improved Yasutomi Pressure-Viscosity Relationship on the Elastohydrodynamic Line Contact Problem", International Scholarly Research Notices, vol. 2013, pp. 1-7, 2013.

[15] J. S. Issa and W. Habchi, "Influence of Realistic Lubricant Density-Pressure Dependence on the Stiffness of Elastohydrodynamic Lubricated Contacts", Journal of Tribology, vol. 142 (3), pp. 1-20, 2019.

[16] S. Jadhav, G. D. Thakre and S. C. Sharma, "Numerical modeling of elastohydrodynamic lubrication of line contact lubricated with micropolar fluid", J Braz. Soc. Mech. Sci. Eng., vol. 40, 326 (2018).

[17] A. Al-Hamood, Friction and thermal behaviour in elastohydrodynamic lubrication power transmission contacts, PhD thesis, Cardiff University, institute of Mechanics and Advance material, 2015.

[18] K. Chen, L. Zenga, Z. Wu and F. Zheng, "Elastohydrodynamic lubrication in point contact on the surfaces of particle-reinforced composite", AIP Advances, vol. 8 (4), 2018.

[19] T. Almqvist, Numerical simulation of elastohydrodynamic and hydrodynamic lubrication using Navier-stokes and Reynolds equation, Department of mechanical engineering, Lulea University, Sweden, 2001.

[20] P. Chaomleffel, G. Dalmaz and V. Philippe, "Experimental Results and Analytical Predictions of EHL Film Thickness", 33rd Leeds Lyon Symposium on Tribology "Tribology at the Interface", Sep 2006, Leeds, United.

[21] J. Makala, G. Dalmaz, B. Villechaise and J. Chaomleffel, "Experimental investigations of elastohydrodynamic point contacts lubricated with a traction fluid", International Tribology Conference Tribology: Voyaging into the New Millennium, Nagasaki, 2000.